RSC Advances

PAPER

View Article Online
View Journal | View Issue

Cite this: *RSC Adv.*, 2025, **15**, 39554

Spectroscopic investigation of cation effects in U(VI)-NO_3^- complexation in aqueous solutions

Srikanth Nayak *

Understanding and manipulating uranyl speciation in aqueous solutions is critical for advancing chemical separation, sensing, and understanding environmental transport of uranyl. We report on the significant enhancement in the complexation of uranyl with nitrate in aqueous solutions containing quaternary ammonium cations leading to the formation of anionic complexes. We base this on the comparative study of the effect of monovalent cations (Na^+, Li^+, NH_4^+, and $N(CH_3)_4^+$) on the complexation equilibria of uranyl-nitrate in solutions, probed by time-resolved laser induced fluorescence spectroscopy (TRLFS). Lifetime-corrected spectra, obtained by extrapolating the time-resolved spectra to $t = 0$, were used to study speciation to mitigate the effects of variations in the fluorescence lifetimes that depend on extraneous factors such as dynamic quenching. We demonstrate that the lifetime-corrected spectra can be used to determine uranyl speciation in aqueous solutions where the mono-nitrate complex forms, and in acetonitrile with $N(CH_3)_4NO_3$ where di-nitrate and tris-nitrato species are formed. Aqueous solutions containing $N(CH_3)_4^+$ are shown to promote the formation of higher complexes of uranyl compared to other inorganic nitrate salts based on the higher redshift in the spectra, poor fits to the two-component model, and the higher apparent formation constants. Comparing the trends in uranyl speciation in the presence of $N(CH_3)_4^+$ in aqueous and acetonitrile solutions, it is proposed that the quaternary ammonium cations (quats) promote the formation of anionic complexes of uranyl by the ion-association mechanism. These results provide a basis for designing quat-assisted separation systems that target anionic actinide species in aqueous solutions.

Received 22nd August 2025
Accepted 24th September 2025

DOI: 10.1039/d5ra06251a

rsc.li/rsc-advances

Introduction

Complexation of actinides with the different ligands present in aqueous solutions can lead to an intricate speciation of the metal which affects the chemical, geological, and biological processes involving actinide ions.[1–4] While the formation constants for different metal complexes are tabulated in databases, factors affecting the formation constants in different solution media are not clearly understood.[5,6] To understand the behavior of metals in complex solutions containing multiple ionic solutes, coordinating ligands, and high electrolyte concentrations, where a variety of chemical and physical interactions are in effect, detailed studies on the effect of solution components on metal speciation are needed.[7,8]

Formation constants for uranyl nitrate complexes vary widely across studies but are generally low similar to other hexavalent actinides.[5,9–14] Extended X-ray absorption fine structure spectroscopy (EXAFS) studies reveal mono-, di-, and tris-nitrato species of uranyl in concentrated nitric acid, with bidentate coordination of nitrate to uranyl.[15] While distribution studies suggest relatively large formation constants for mono- and di-nitrate species,[16,17] microcalorimetry and potentiometric studies support the formation of mono-nitrate species alone.[18–21] Interestingly, spectroscopic studies have reported differing speciation profiles: some report predominant mono-nitrate species,[19,20] others favor di- and tris-nitrato species.[22,23] Microcalorimetric study of uranyl nitrate complexation suggests that both inner and outer sphere complexes are formed in aqueous solutions,[21] which could explain the discrepancies between thermodynamic and spectroscopic measurement of complexation as spectroscopic methods are mainly sensitive to inner sphere complexation. In addition, these experiments differed in the medium conditions such as ionic strength, pH, and the salt used, highlighting the need for a better understanding of medium effects on uranyl-nitrate complexation in aqueous solutions.

The weak interaction between uranyl and nitrate ions in aqueous solutions typically necessitates a high nitrate concentration, and thereby a high background cation concentration, to study the uranyl-nitrate complexation reaction. This raises the question regarding the role played by the background cations in the complexation of uranyl. Although relatively less studied, the background cations present in the solution are known to influence metal–ligand complexation and their solvation. For example, "salting out" effects in solvent extraction have been

Chemical Sciences and Engineering Division, Argonne National Laboratory, Lemont, IL 60439, USA. E-mail: snayak@anl.gov

attributed to the effect of cations on ion hydration.[24,25] Counter-cation effects in the synthesis of molecular compounds of actinides have also been reported.[26–28] These results challenge the notion that counter-cations are just charge-balancing species and support their active role in affecting metal speciation in solutions.[25,29,30] An interesting example of cation effects is observed in the formation of ternary association complexes of alkaline earth cations and anionic actinide complexes in alkaline solutions and brines.[31,32] The formation of these ion-association complexes has been linked to the unexpectedly high solubility of actinides in brines containing alkaline earth cations.[32] Similarly, solubility of uranyl in alkaline solutions is increased in the presence of quats compared to other cations.[33,34] Quats have also been shown to influence the redox equilibrium of Np(VI) species in aqueous chloride solutions, and this effect has been attributed to specific interactions between the actinyl and the quats.[35] Quats promote the formation tris-nitrato complex of uranyl in acetonitrile and an ionic liquid, 1-butyl-3-methylimidazolium bis(trifluoromethylsulfonyl) imide.[36,37] Quats are used in solvent extraction of metals and as phase transfer catalysts primarily due to their ability to form ion-association complexes.[24,38] Given that the anionic complexes of actinides are formed in organic solutions with quats, it is important to understand whether complexation of actinides with anions in aqueous solutions is enhanced in the presence of quats.

We hypothesize that the quats uniquely drive the formation of anionic complexes of actinyls by the formation of ion-association complexes. To test this, we study uranyl-nitrate complexation in the presence of different monovalent nitrate salts ($NaNO_3$, $LiNO_3$, NH_4NO_3, and $N(CH_3)_4NO_3$) in aqueous solutions using TRLFS. TRLFS has been used to understand uranyl speciation in various matrices, particularly due to its sensitivity to low concentrations of uranyl and its temporal and spectral sensitivity to uranyl speciation.[39] We develop our method based on lifetime-corrected luminescence spectra and benchmark it by studying the speciation of uranyl in aqueous solutions containing $NaNO_3$/$NaClO_4$ at fixed ionic strength and in acetonitrile solutions containing $N(CH_3)_4NO_3$. We show the formation of mono-nitrate complex and tris-nitrato complexes in the aqueous and acetonitrile solutions, respectively, with formation constants that match the literature-reported values. We then the extend the study to aqueous solutions containing $NaNO_3$, $LiNO_3$, NH_4NO_3, and $N(CH_3)_4NO_3$ without constraining the ionic strength of the solutions. All the spectra, except those recorded for $N(CH_3)_4NO_3$ solutions, could be deconvoluted into two components – UO_2^{2+} and $UO_2NO_3^{+}$. Despite the poorer fits to the spectra and the mass action model in the case of $N(CH_3)_4NO_3$ solutions, the apparent formation constants obtained show an increase in the uranyl-nitrate complexation. Based on the similarities of trends in lifetimes and lifetime-corrected spectra in aqueous and acetonitrile solutions containing $N(CH_3)_4NO_3$, we ascribe the increased complexation in aqueous solution to the formation of anionic complex of uranyl driven by the quat. Controlling uranyl speciation in aqueous solutions by the addition of different salt cations provides an important handle in metal separation processes. Effect of quats on the speciation of uranyl could be leveraged in the sensing and separation technologies for uranyl by using quats as hold-back agents or stripping agents to enhance the separation factors.[40] Thus, these findings not only demonstrate the critical role of solution environment in modulating uranyl-nitrate complexation but also open new avenues for the design of advanced extraction systems.

Experimental

Caution! *U-238 is an alpha-emitting isotope. All experiments described here were performed in specially designed laboratories with negative pressure fume hoods, using strict radiological controls*.

$UO_2(NO_3)_2\cdot 6H_2O$ was obtained from Argonne National Laboratory stock. $LiNO_3$, anhydrous (≥99%), $NaNO_3$ ACS reagent (≥99%), NH_4NO_3 (≥99%), were obtained from Thermo Scientific Chemicals. $N(CH_3)_4NO_3$ (≥95%), $NaClO_4$ (≥98%), and anhydrous acetonitrile were obtained from Sigma-Aldrich. HNO_3 was obtained from Fisher Chemicals. Stock solutions of uranyl nitrate in nitric acid were prepared in volumetric flasks by weighing an appropriate amount of $UO_2(NO_3)_2\cdot 6H_2O$. Stock solutions of nitrate salts in 18.2 MΩ cm water were also prepared in volumetric flasks and filtered with 0.22 μm PTFE filters. Aqueous samples were prepared by adding the appropriate volumes of the stock solutions to yield 0.2 mM of $UO_2(NO_3)_2$ and 20 mM of HNO_3. Samples in acetonitrile were prepared by mixing stock solutions of $UO_2(NO_3)_2\cdot 6H_2O$ and $N(CH_3)_4NO_3$ dissolved in acetonitrile. The solutions were contained in air-tight glass vials and stored under nitrogen.

TRLFS data was collected on an Edinburgh Instruments FLS1000 photoluminescence spectrometer equipped with a tunable laser (Opolette UX10230) operating at a repetition rate of 20 Hz, and a PMT detector (PMT900, Edinburgh Instruments) in multichannel scaling mode. Excitation wavelength and emission bandwidth were fixed at 355 nm and 0.75 nm, respectively. The samples were contained in 10 mm path-length quartz cuvettes and stirred with a magnetic stirrer. The temperature was controlled by placing the cuvette in an air-cooled sample holder. All the measurements were conducted at 20 °C. Fluorescence decays were measured for 30 s each at emission wavelengths 460–610 nm, with a step size of 2 nm. TRLFS of $UO_2(NO_3)_2\cdot 6H_2O$ was measured in 2 mm quartz capillary with an emission bandwidth of 0.06 nm.

Model equations

Fluorescence decays were found to be mono-exponential and modeled as such according to eqn (1a). $I^0(\lambda)$, $\tau(\lambda)$, and b are the intensity at $t = 0$ (referred to as the lifetime-corrected spectrum), lifetime, and background term, respectively. The background term was fixed for a given sample across the emission wavelengths and was found to be <0.2% of the maximum signal.

$$I(\lambda,t) = I^0(\lambda)e^{-t/\tau(\lambda)} + b \quad (1a)$$

$$I^0(\lambda) = A_1 \times I_1{}^0 + A_2 \times I_2{}^0 \quad (1b)$$

$$= A_1 \times \sum_{k=1}^{6} \frac{a_k}{1+\left(\frac{\lambda-\lambda_k}{\sigma_k}\right)^2} + A_2 \times \sum_{k=1}^{6} \frac{a_k}{1+\left(\frac{\lambda-(\lambda_k+\Delta_2)}{\sigma_k s_2}\right)^2} \quad (1c)$$

$I^0(\lambda)$ of the aqueous solutions were fit to a two-component model according to eqn (1c). The assumptions behind this model are: (1) all the spectra can be described as sums of component spectra weighted by their prevalence and (2) the spectra of the two components are identical except for a relative spectral shift and broadening. In this model, the spectra for each component is modeled as a sum of six Lorentzian peaks with a_k, λ_k, and σ_k corresponding to the amplitude, center, and width of k^{th} peak respectively, as parameters. Parameter Δ_2 refers to the spectral shift of the second component with respect to the first. Similarly, s_2 refers to the relative spectral broadening of the second component. Each of the six Lorentzian peaks in the second component are shifted and broadened by the same Δ_2 and s_2 with respect to the first component. Prefactors in eqn (1b) and (1c), A_1 and A_2, correspond to the contribution of the first and the second components to the spectra. We fit all the spectra obtained in the aqueous phase experiments to this model so that the component spectra ($I_1{}^0$ and $I_2{}^0$) are the same in all fits, *i.e.*, only A_1 and A_2 vary between the samples. All least squares fits were obtained using the lmfit package.[41]

The $I^0(\lambda)$ spectra of uranyl in acetonitrile solutions of $N(CH_3)_4NO_3$ were found to have an isosbestic point and not change appreciably above $\frac{[UO_2(NO_3)_2]}{[N(CH_3)_4NO_3]} = 1$. Accordingly, the spectra at the extremes of titration ($[N(CH_3)_4NO_3] = 0$ mM and 1 mM) were fit to eqn (2a) and the spectra at the intermediate $[N(CH_3)_4NO_3]$ values were fit as linear combinations of the spectra at the end points (eqn (2b)).

$$I^0 = A \times \sum_{k=1}^{6} \frac{a_k}{1+\left(\frac{\lambda-\lambda_k}{\sigma_k}\right)^2} \quad (2a)$$

$$I^0(\lambda,[N(CH_3)_4NO_3]) = yI^0(\lambda,[N(CH_3)_4NO_3] = 0\text{ mM}) + (1-y)\, I^0(\lambda,[N(CH_3)_4NO_3] = 1\text{ mM}) \quad (2b)$$

Results and discussion

Formation constants for weak metal complexes are typically obtained at high concentrations of ligand (salt), and the ionic strength of the solutions is held constant using a non-coordinating anion such as perchlorate to circumvent the challenges in modeling activity coefficients. One of the cations of particular interest in this study, $N(CH_3)_4{}^+$, has low solubility in perchlorate solutions. Consequently, we first studied the complexation of uranyl with nitrate in (a) aqueous sodium salt solutions with constant ionic strength and (b) acetonitrile solutions with $N(CH_3)_4NO_3$ to validate the analysis, and then expanded the methodology to study the effect of the cations on the uranyl-nitrate complexation in aqueous solutions.

U(VI)-$NO_3{}^-$ complexation at constant ionic strength in aqueous solutions

Representative TRLFS data of uranyl in nitrate-perchlorate mixtures displayed in Fig. 1 show the broadening of spectral features with increasing nitrate concentration. Fluorescence decays of 510 nm emission line are shown for some of the aqueous solutions in Fig. S1. Regardless of the solution composition, the decay curves were found to be mono-exponential although the lifetimes depend on the solution composition. Single lifetimes in the presence of multiple species has been suggested to be due to fast exchange between the excited states of the different species.[42,43]

Fluorescence lifetimes ($\tau(\lambda)$) and lifetime-corrected fluorescence spectra ($I^0(\lambda)$ were obtained by fitting the TRLFS data to eqn (1a) and results are shown in Fig. 2. There is a monotonic decrease in the fluorescence lifetimes across the emission wavelengths as the concentration of nitrate is increased. Interestingly, in the absence of any salts, τ is ~2.21 μs at 510 nm, which is significantly smaller than that obtained at 4 M $NaClO_4$, $\tau \sim 3.45$ μs. Given the spectroscopic evidence that the perchlorate anion is not coordinated to uranyl,[44,45] this shows that $\tau(\lambda)$ by itself is not a reliable measure of complexation. Lifetime of uranyl in aqueous solution is affected by multiple factors such as ground- and excited-state complexation, collisional quenching by solvent and other molecules, and the fast exchange between the excited-state species. Thus, to understand the effect of salts on the complexation equilibria, it is preferable to study the spectral features that are independent of the fluorescence decay properties. So we develop a method to obtain speciation using $I^0(c,\lambda)$, obtained by fitting the TRLFS to eqn (1a).

We used least-squares peak fitting to analyze the variations in lifetime-corrected spectra with solution composition. Lifetime-corrected spectra are assumed to be linear combinations of the underlying component spectra. Since the spectrum of $UO_2{}^{2+}$ species is known from perchlorate solutions with negligible concentrations of $NO_3{}^-$, the task is to obtain the spectrum of the other components in solution. As the symmetric stretching mode of O=U=O is not perturbed by the nitrate complexation,[46,47] the vibronic progression observed in the fluorescence spectrum, particularly the spacing between the peaks, is not expected to differ significantly due to nitrate complexation. Taking this into account, we model the spectra of the nitrate complexes of uranyl to be similar to the spectra of the $UO_2{}^{2+}$ species, but with a different spectral broadening and a constant shift in the peak centers. On the basis of the spectrum of the bare uranyl (aquo complex), we fit each component spectra to a sum of six Lorentzian peaks. All the fit parameters in eqn (1c) were obtained by a global fit of the spectra and are shown in Table 1. Only the A_1 and A_2 terms, corresponding to the contribution of the first and the second components, are allowed to vary freely for all samples. The results of the fit for certain compositions are shown in Fig. 3. Excellent fits were obtained at all the compositions, with a reduced chi-squared statistic, $\chi^2 = 1.1 \times 10^{-6}$. The weak peak at ~470 nm is not well captured by the model possibly due to interference from

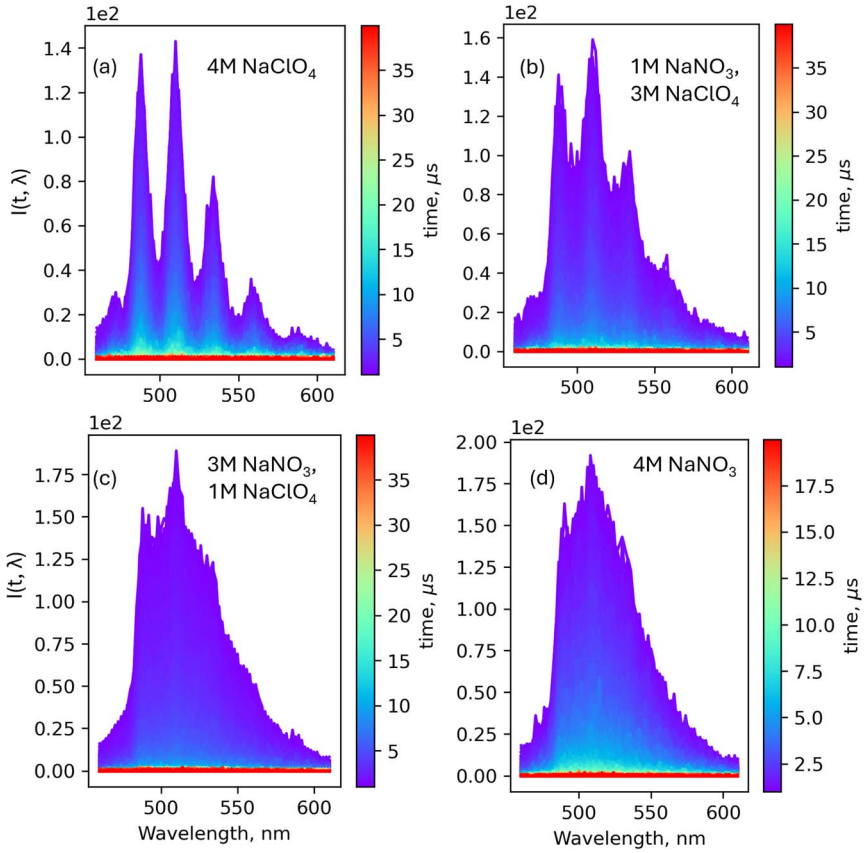

Fig. 1 TRLFS of 0.2 mM $UO_2(NO_3)_2$ in 20 mM HNO_3 and (a) 4 M $NaClO_4$, (b) 1 M $NaNO_3$ and 3 M $NaClO_4$, (c) 3 M $NaNO_3$ and 1 M $NaClO_4$, and (d) 4 M of $NaNO_3$. Color bars next to the plots correspond to the time after excitation at which the spectra are collected. TRLFS were obtained with the laser excitation wavelength fixed at 355 nm.

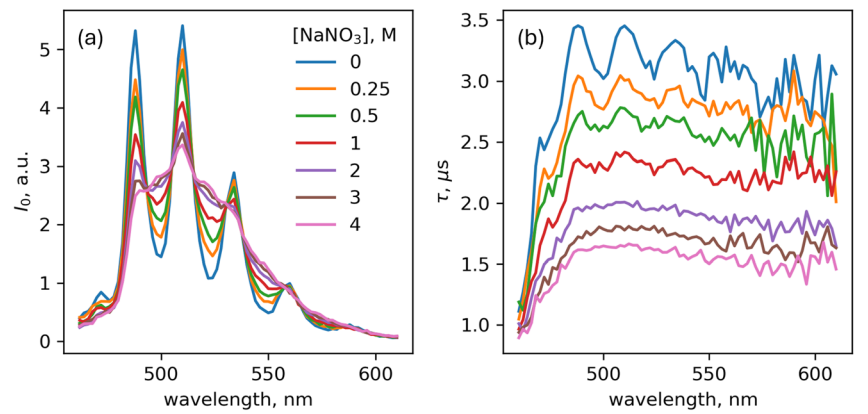

Fig. 2 (a) The lifetime-corrected spectra and (b) the lifetimes of uranyl fluorescence decay in solutions of $NaNO_3$ with a constant ionic strength of 4 M, obtained by adjusting $NaClO_4$ concentration. Lifetimes (τ) and the lifetime-corrected spectra (I^0) were obtained by fitting the TRLFS to eqn (1a).

the tail of the strong peak centered at 488 nm. Fit parameters are tabulated in Table 1. The fit value for Δ_2 of 11.06 nm indicates the redshift of the second component with respect to the first component. Further, the value of $s_2 = 2.36$ shows that the spectrum of the second component is also slightly broadened compared to the first component.

$$UO_2^{2+} + NO_3^- \overset{\beta}{\rightleftharpoons} UO_2(NO_3)^+ \quad (3a)$$

$$\frac{[UO_2^{2+}]}{[U(VI)_{total}]} = \frac{1}{1 + \beta[NO_3^-]} \quad (3b)$$

Table 1 Fit parameters for the six Lorentzian peaks obtained from fitting the lifetime-corrected spectra to eqn (1c). λ_k, σ_k, and a_k are peak centers, widths, and amplitudes, respectively. Fit values of Δ_2 and s_2 are 11.06 ± 0.09 nm and 2.35 ± 0.07, respectively

Peak (k)	λ_k, nm	σ_k, nm	a_k
1	469.7 ± 0.60	2.58 ± 0.83	0.4 ± 0.09
2	488.04 ± 0.07	3.98 ± 0.03	4.62 ± 0.07
3	510.00 ± 0.07	4.94 ± 0.11	5.70 ± 0.07
4	533.6 ± 0.15	5.77 ± 0.25	3.00 ± 0.06
5	559.4 ± 0.46	6.21 ± 0.81	0.92 ± 0.06
6	587.9 ± 2.59	10.67 ± 4.45	0.17 ± 0.05

$$\frac{[UO_2(NO_3)^+]}{[U(VI)_{total}]} = \frac{\beta[NO_3^-]}{1+\beta[NO_3^-]} \quad (3c)$$

The presence of two spectral components indicates that the solutions contain two dominant U(VI) species. Based on this, the complexation of uranyl with nitrate in aqueous solutions was modeled according to eqn (3), considering two chemical species at equilibrium, UO_2^{2+} and $UO_2(NO_3)^+$, corresponding to the two spectral components.The proportions of the two spectral components $\left(\frac{A_1}{A_1+A_2} \text{ and } \frac{A_2}{A_1+A_2}\right)$ obtained by fitting $I^0(\lambda)$ are shown in Fig. 3(d). Good fits to these component fractions were obtained by assigning the spectral components to UO_2^{2+} and $UO_2(NO_3)^+$ species and applying eqn (3). This confirms that uranyl speciation in $NaNO_3$ solutions is mainly in the form of UO_2^{2+} and $UO_2(NO_3)^+$. We obtain a formation constant, $\log\beta = -0.44 \pm 0.01$, comparable to the values in the range of −0.4 to −0.7 reported for similar conditions using spectrophotometry and distribution studies (Table S1).[16,19,21,48]

Uranyl-nitrate complexation in $N(CH_3)_4NO_3$/acetonitrile solutions

Formation of successive complexes of U(VI) with NO_3^- ($UO_2(NO_3)_i^{2-i}$, $i = 1, 2, 3$) in acetonitrile in the presence of quaternary ammonium nitrates has been shown.[36,37] To probe whether TRFLS can capture the speciation in systems containing di-, and tris-nitrato species of U(VI) we studied the TRLFS of complexes formed in acetonitrile upon titrating solutions of $UO_2(NO_3)_2 \cdot 6H_2O$ with $N(CH_3)_4NO_3$. The fluorescence decays at all the concentrations showed mono-exponential behavior as shown in Fig. S2, and the corresponding $I^0(\lambda)$ and $\tau(\lambda)$ are displayed in Fig. 4. Upon the addition of $N(CH_3)_4NO_3$, the spectra show subtle changes of fluorescence intensity in the region between the peaks, decreasing around 480 nm and increasing around 520 and 545 nm. The peaks at ~510, ~532, and ~556 nm broaden while those at ~471, ~490, and ~584 narrow with

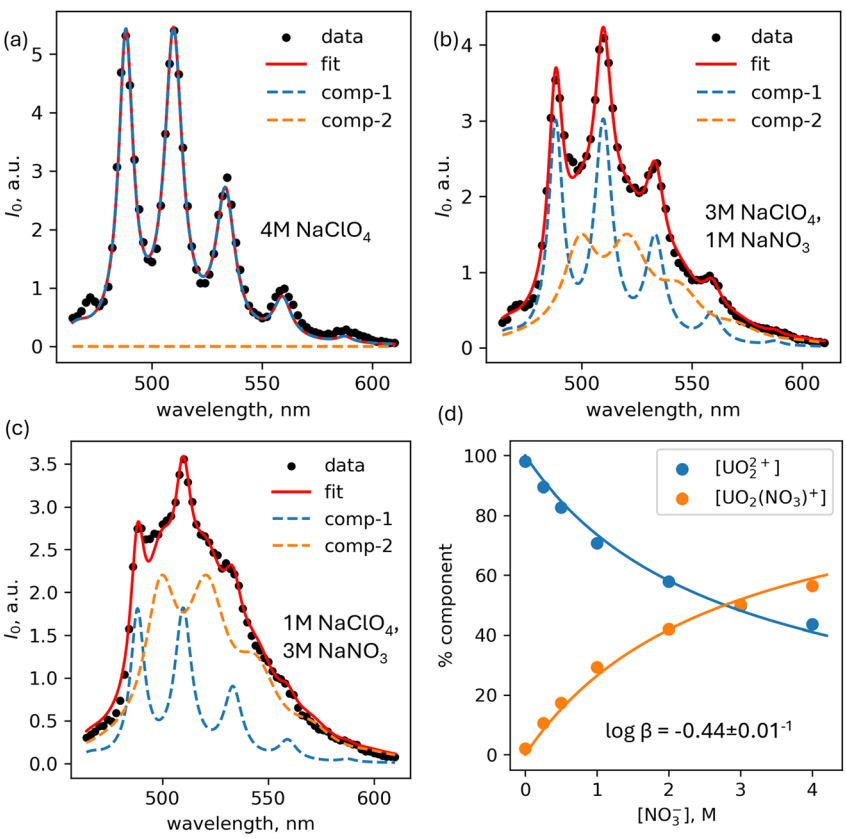

Fig. 3 Lifetime-corrected spectra (I^0) fit to the two-component model (eqn (1c)), shown for 0.1 mM $UO_2(NO_3)_2$, 20 mM HNO_3 solutions with (a) 4 M $NaClO_4$, (b) 1 M $NaNO_3$ and 3 M $NaClO_4$, (c) 3 M $NaNO_3$ and 1 M $NaClO_4$, and (d) the component fractions fit to eqn (3). The component spectra are shown with dashed lines.

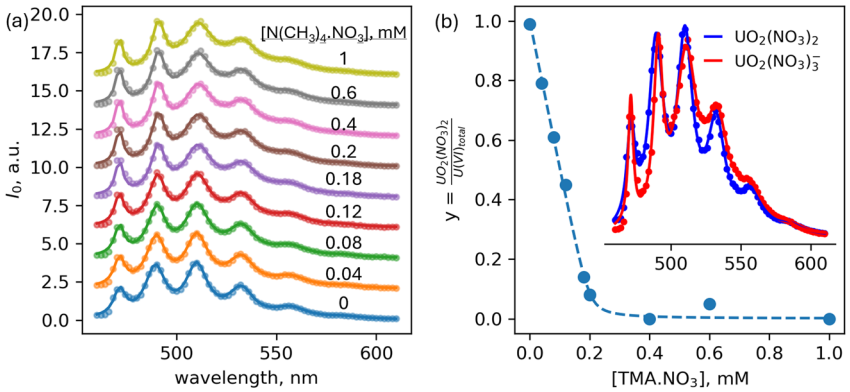

Fig. 4 (a) $I^0(\lambda)$ spectra of solutions containing 0.2 mM $UO_2(NO_3)_2 \cdot 6H_2O$ in acetonitrile and varying concentrations of $N(CH_3)_4NO_3$ shown along with their corresponding fits to eqn (2b). (b) Fraction of $UO_2(NO_3)_2$ component in the I^0 spectra in (a) obtained by fits to eqn (2b). The solid line is obtained by fits to the mass-action model shown in eqn (4a). The inset plot shows the spectra of $UO_2(NO_3)_2$ and $UO_2(NO_3)_3^-$ obtained from the spectra at $[N(CH_3)_4NO_3] = 0$ and 1 mM, respectively, along with their fits to eqn (2b).

increasing $N(CH_3)_4NO_3$ concentration. These variations in peak widths could be due to the hydration of the complexes, but the precise mechanism determining the widths are not clear.[49] There is also an isosbestic point around 500 nm indicating that there are two major fluorescing species. Further, the spectral shape does not greatly vary upon increasing the ratio of $N(CH_3)_4NO_3$ to $UO_2(NO_3)_2 \cdot 6H_2O$ to above 1, indicating the formation of tris-nitrato species. This is in agreement with the formation of $UO_2(NO_3)_3^-$ in acetonitrile in the presence of 1 : 1 $UO_2(NO_3)_2 : N(C_4H_9)_4NO_3$ shown by EXAFS and UV-vis studies.[36] Predominance of $UO_2(NO_3)_2$ in acetonitrile solutions containing 1 : 2 U(VI) : NO_3^- has been shown by a combined EXAFS, UV-vis and DFT study.[37] Accordingly, we infer that the other species in these solutions is $UO_2(NO_3)_2$. Thus, formation of higher nitrate complexes of U(VI) in acetonitrile shifts the fluorescence spectral intensity to higher wavelengths resembling the same effect in aqueous nitrate solutions. The spectra at $[N(CH_3)_4NO_3] = 0$ and 1 mM were independently fit to a sum of six Lorentzian peaks (eqn (2a)) and the fit parameters are provided in Table S2. The peak positions from the fits are within error for the two species, but the trend in peak widths reflects the increasing fluorescence intensity at higher wavelengths for the $UO_2(NO_3)_3^-$ species. We fit the spectra at the intermediate concentrations of $N(CH_3)_4NO_3$ as linear combinations of the fit-spectra at $[N(CH_3)_4NO_3] = 0$ and 1 mM (eqn (2b)). Variation of the proportion of the first component ($UO_2(NO_3)_2$ in the spectra, y, is shown in Fig. 4(b). There is an almost linear decrease in y with $[N(CH_3)_4NO_3]$ reaching a value of 0 near $\frac{[U(VI)]_{total}}{[N(CH_3)_4NO_3]_{total}} = 1$ indicating near complete conversion of U(VI) to $UO_2(NO_3)_3^-$.

$$UO_2(NO_3)_2 + N(CH_3)_4NO_3 \overset{\beta_{23}}{\rightleftharpoons} N(CH_3)_4UO_2(NO_3)_3 \quad (4a)$$

$$[U(VI)]_{total} = [UO_2(NO_3)_2](1 + \beta_{23}[N(CH_3)_4NO_3]) \quad (4b)$$

$$[N(CH_3)_4NO_3]_{total} = [N(CH_3)_4NO_3](1 + \beta_{23}[UO_2(NO_3)_2]) \quad (4c)$$

$$y = \frac{[UO_2(NO_3)_2]}{[U(VI)]_{total}} \quad (4d)$$

$$y^2 + \left(\frac{\left(1 + \beta_{23}\left([N(CH_3)_4NO_3]_{total} - [U(VI)]_{total}\right)\right)}{\beta_{23}[U(VI)]_{total}}\right) \quad (4e)$$

The y values obtained from the above TRFLS results were fit to a mass action model for the equilibrium between $UO_2(NO_3)_2$ and $UO_2(NO_3)_3^-$, shown in eqn (4a). Using the mass balance equations (eqn (4b) and (4c)), we obtain a quadratic equation for y, the fraction of $UO_2(NO_3)_2$ in the solution. Apparent formation constant for $N(CH_3)_4UO_2(NO_3)_3$ in acetonitrile (β_{23}) was obtained by solving eqn (4e) for y and fitting the results from the $I^0(\lambda)$ fits to eqn (2b). From this procedure we obtain a fit value of $\beta_{23} = 6.0 \pm 2.4 \times 10^5$ M^{-1}, although due to near complete conversion of $UO_2(NO_3)_2$ this value should be considered as a lower estimate for β_{23} in acetonitrile. A complete conversion of U(VI) to $UO_2(NO_3)_3^-$ above 1 : 3 ratio of U(VI) : NO_3^- was also observed with UV-vis and EXAFS study of U(VI)-NO_3^- complexation in acetonitrile with $N(C_4H_9)_4NO_3$, starting with $UO_2(ClO_4)_2 \cdot nH_2O$.[37] From their fits to the UV-vis data, the authors report $\log \beta_2 = 15.0 \pm 0.5$ and $\log \beta_3 = 20.0 \pm 0.2$ for the formation of $UO_2(NO_3)_2$ and $UO_2(NO_3)_3^-$, respectively. The formation constant for $UO_2(NO_3)_3^-$ from $UO_2(NO_3)_2$ can be estimated as $\log \beta_3 - \log \beta_2 = 5$, which is in agreement with the value from our fits to the $I^0(\lambda)$ spectra.

The fluorescence lifetimes were found to initially increase from ~9.5 μs to ~12.9 μs at 1 : 1 U(VI) : $N(CH_3)_4NO_3$ coinciding with the formation of $UO_2(NO_3)_3^-$, but then gradually reduced to ~9.9 μs at 1 : 5 U(VI) : $N(CH_3)_4NO_3$ (Fig. S3(a), possibly due to the quenching effect of $N(CH_3)_4NO_3$. The coordination shell of the dinitrate species has been suggested to be completed by two water molecules with the nitrates binding in bidentate fashion.[37] Thus, the formation of $UO_2(NO_3)_3^-$ species would involve loss of water molecules from the coordination shell. The increase in fluorescence lifetimes with the formation of

$UO_2(NO_3)_3^-$ could be associated with the changes in coordination environment around U(VI). Much higher lifetimes are obtained in acetonitrile medium compared to aqueous solutions implying the role of the solvent in quenching of uranyl fluorescence. The Stern–Volmer plot showing the variation of fluorescence decay rates (as inverse lifetimes) with the concentration of $N(CH_3)_4NO_3$ in acetonitrile is shown in Fig. S3(b). At $N(CH_3)_4NO_3 : UO_2(NO_3)_2 \cdot 6H_2O$ less than one, the lifetimes gradually increase due to the formation of tris-nitrato complex. At $N(CH_3)_4NO_3 : UO_2(NO_3)_2 \cdot 6H_2O$ greater than one, the lifetimes decrease, showing a linear behavior in the Stern–Volmer plot, indicating the presence of dynamic quenching. Observation of a single lifetime suggests a fast equilibrium of the excited state populations of the two species, similar to that observed in aqueous solutions.

Comparison of spectra obtained for different U(VI)-NO_3^- species

Fluorescence properties of higher nitrate complexes of U(VI) have been studied in crystalline and solution state.[36,49–51] For comparison, we measured the TRLFS of $UO_2(NO_3)_2 \cdot 6H_2O$ in powder form. The $I^0(\lambda)$ obtained from the analysis of the time-resolved spectra are shown in Fig. 5(a) and the corresponding $\tau(\lambda)$ is shown in Fig. S4. The spectrum shows intense peaks centered around ~488 nm, ~510 nm, ~532 nm, ~560 nm, and ~588 nm, which overlap with the peak positions of UO_2^{2+} in aqueous solutions (Fig. 3 and Table 1). The fluorescence lifetimes increase steeply with the emission wavelength to a value of ≈0.7 ms, similar to the values reported earlier.[49]

Fig. 5(b) compares the $I^0(\lambda)$ obtained for the different complexes of U(VI) with NO_3^-: UO_2^{2+} and $UO_2(NO_3)^+$ (obtained from aqueous solutions with), $UO_2(NO_3)_2 \cdot 6H_2O$ (in solid state), and $UO_2(NO_3)_3^-$ (obtained from acetonitrile solutions with $N(CH_3)_4NO_3$). The spectral features show a high degree of overlap for the different complexes, but when comparing spectra of the complexes in the same solvent, there is a trend of increasing intensity towards higher wavelengths with increasing number of NO_3^- complexed to U(VI). Interestingly, the peak at ~470 nm is present in UO_2^{2+} and $UO_2(NO_3)_3^-$, but is absent in $UO_2(NO_3)_2 \cdot 6H_2O$. The other four intense peaks overlap significantly in position for UO_2^{2+} and $UO_2(NO_3)_2 \cdot 6H_2O$, but the peak intensities vary relatively. The spectrum of the $UO_2(NO_3)_3^-$ obtained in acetonitrile appears slightly red-shifted compared to the UO_2^{2+} spectrum. The spectrum for $UO_2(NO_3)^+$, obtained from fits to the aqueous solutions data appears relatively less-resolved in peaks, indicating that the width of the peaks depends on the solvent.

Cation effect on U(VI)-NO_3^- complexation in aqueous solutions

Having verified that the I^0 spectra can be used to obtain speciation of uranyl in nitrate solutions, we investigated the effect of cations on uranyl-nitrate complexation in aqueous solutions. TRLFS were collected on solutions of uranyl nitrate in the presence of increasing concentrations of one of $NaNO_3$, $LiNO_3$, NH_4NO_3, and $N(CH_3)_4NO_3$ as the background electrolyte. Four representative spectra are shown in Fig. S5. While the solutions containing Na^+, Li^+, or NH_4^+ have similar TRLFS, those containing $N(CH_3)_4^+$ were relatively more quenched. The lifetimes as a function of emission wavelength and solution composition, extracted by fitting the TRLFS to eqn (1a) are shown in Fig. 6. In the absence of salt, lifetimes rise steeply from ~1.2 μs at ~470 nm emission to ~2.2 μs at 490 nm and has a slight downward trend at longer wavelengths (Fig. 6(a), blue trace). Lifetimes appear to peak coinciding with peaks in the emission spectra. With increasing $[NaNO_3]$ the lifetimes decrease gradually and the peaks disappear. This appears similar to the variation of emission spectra where the peaks broaden with increasing $[NaNO_3]$ (Fig. 2(a)). Solutions containing $LiNO_3$ and NH_4NO_3 showed similar trends in lifetimes (Fig. S6). For the $N(CH_3)_4NO_3$ solutions, the lifetime decreases rapidly at low concentrations of the salt, reaches a minimum at about 2 M and then increases slightly to ~0.79 μs (Fig. S7). The increase in the lifetimes at high $N(CH_3)_4NO_3$ is unique compared to other inorganic nitrate salts. Although these variations could be due to the varying uranyl speciation in solutions, because of the

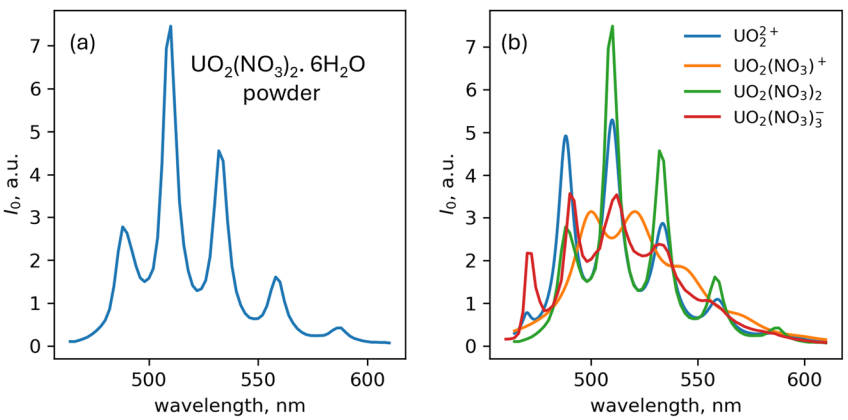

Fig. 5 (a) Lifetime-corrected spectra (I^0) obtained by fitting eqn (1a) to the TRLFS data of solid $UO_2(NO_3)_2 \cdot 6H_2O$, and (b) comparison of $I^0(\lambda)$, normalized by the area under the spectra, for the different U(VI)-NO_3^- complexes and compounds: UO_2^{2+}, $UO_2(NO_3)^+$ (from fitting aqueous solution spectra), $UO_2(NO_3)_2 \cdot 6H_2O$ (powder), and $UO_2(NO_3)_3^-$ (from acetonitrile solutions).

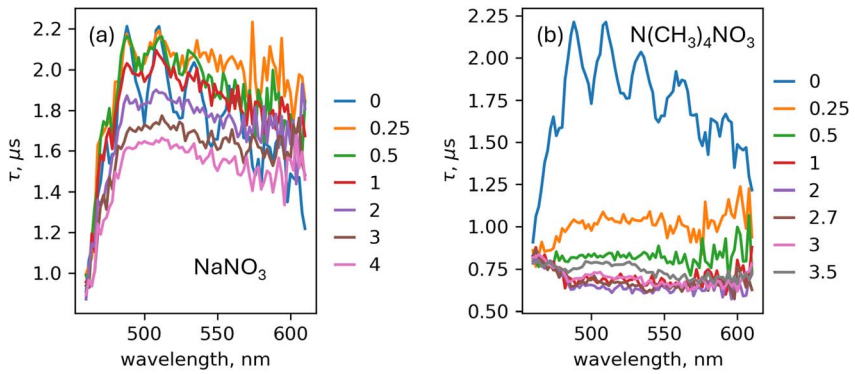

Fig. 6 Variations in the lifetimes ($\tau(\lambda)$) of the uranyl species in varying concentrations of (a) $NaNO_3$ and (b) $N(CH_3)_4NO_3$, obtained by fitting the TRLFS data to eqn (1a). Legend entries refer to the concentration of the salt in the samples in *M*.

challenges mentioned above in analysing the lifetimes, we focus on the lifetime-corrected spectra to quantify uranyl speciation in these solutions.

Variation of I^0 with the salt concentration in $NaNO_3$ and $N(CH_3)_4NO_3$ solutions is shown in Fig. 7(a and b) and the salt dependence for two salt concentrations are shown in Fig. 7(c and d). I^0 spectra for the $LiNO_3$ and NH_4NO_3 solutions as a function of salt concentration are also shown in Fig. S8. These results show that the spectra broaden with increasing salt concentration which we attribute to a change in the uranyl speciation. Interestingly, $N(CH_3)_4NO_3$ solutions show a marked difference in the spectra compared to the other nitrate solutions as they show a higher redshift and are more broadened indicating a clear effect of the cations on uranyl-nitrate complexation. These trends indicate a higher uranyl-nitrate complexation in the presence of $N(CH_3)_4^+$ ions. Fits to the $I^0(\lambda)$ spectra were performed as described for the $NaNO_3$ + $NaClO_4$ solutions. While good fits were obtained for the solutions containing $NaNO_3$, $LiNO_3$, or NH_4NO_3, fits were poorer for solutions containing high concentrations of $N(CH_3)_4NO_3$ (Fig. 8). This

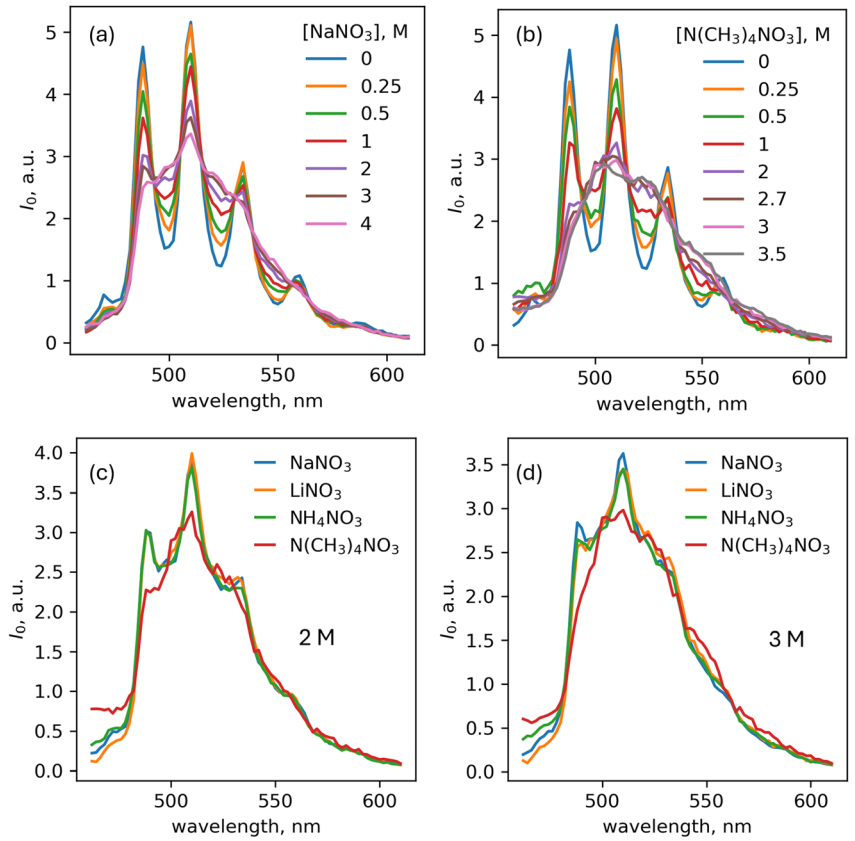

Fig. 7 Lifetime-corrected spectra (I^0) obtained by fitting eqn (1a) to the TRLFS data of solutions with 0.2 mM $UO_2(NO_3)_2$, 20 mM HNO_3, and (a) varying [$NaNO_3$], (b) varying [$N(CH_3)_4NO_3$], (c) different salts at 2 M salt concentration, and (d) different salts at 3 M of salt concentration.

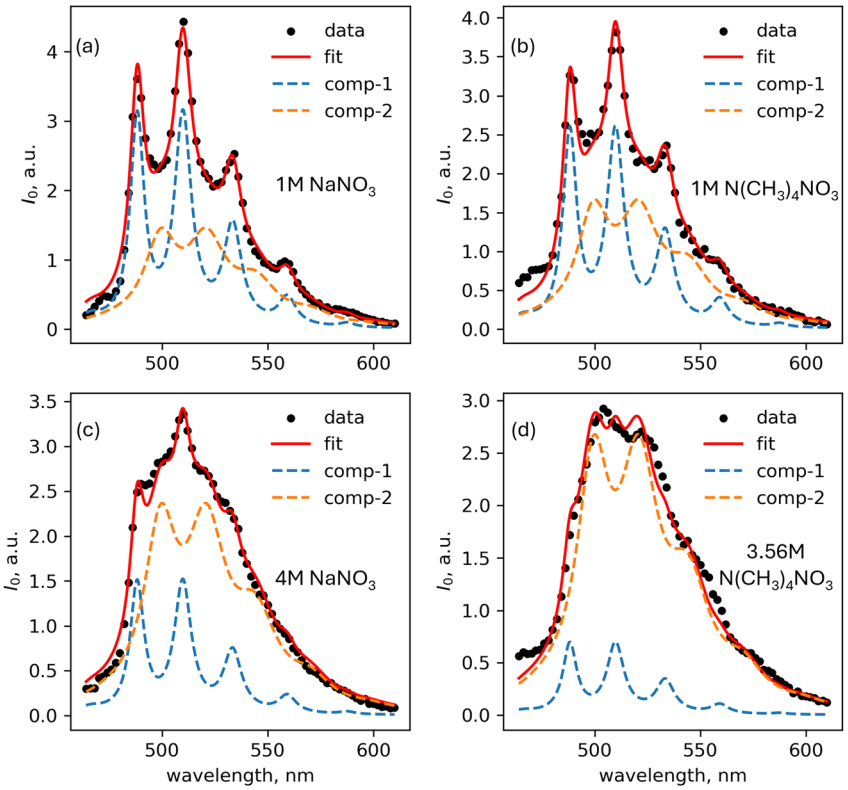

Fig. 8 Lifetime-corrected spectra ($I^0(\lambda)$) fit to the two-component model (eqn (1c)), shown for 0.2 mM $UO_2(NO_3)_2$, 20 mM HNO_3 solutions with (a) 1 M $NaNO_3$, (b) 1 M $N(CH_3)_4NO_3$ (c) 4 M $NaNO_3$, and (d) 3.5 M of $N(CH_3)_4NO_3$. The spectra of the components are shown with dashed lines.

indicates that the two-component model is not adequate to describe the speciation of uranyl in $N(CH_3)_4NO_3$ solutions.

The proportion of the two spectral components (A_1 and A_2) obtained from the fits to the lifetime-corrected spectra are shown in Fig. 9. A_1 decreases while A_2 increases with increasing nitrate concentration for all salt solutions studied. The speciation of uranyl is clearly different in $N(CH_3)_4^+$ solutions compared to that in Na^+, NH_4^+, and Li^+ solutions. To quantify the effects of cations on the complexation of uranyl with nitrate, we applied a simple mass-action model shown in eqn (3), using just the concentrations of ions. The fits are shown in Fig. 9 as solid lines, and the fit parameters are shown in Table 2. While good fits were obtained for Na^+, NH_4^+, and Li^+ solutions, fits to the $N(CH_3)_4^+$ solutions were poorer, showing significant deviations throughout the concentration range. The $\log\beta$ values obtained from the fits are between -0.41 and -0.46 for solutions with Na^+, Li^+, and NH_4^+, but it is -0.16 for the $N(CH_3)_4^+$ solutions. Interestingly, the formation constants obtained for the Na^+ solutions with constant (-0.44 ± 0.01) or changing solution ionic strengths (-0.46 ± 0.01) are similar, suggesting that the activity coefficient corrections do not greatly affect the formation constants. The $N(CH_3)_4^+$ system stands out because of the high formation constant and poorer fits to the mass-action model. This, along with the anomalous shift observed in the lifetime-corrected spectra, suggests that $N(CH_3)_4^+$ uniquely affects the complexation of uranyl with nitrate compared to the other cations. Our attempts to improve the fits to the $I^0(\lambda)$ of aqueous solutions containing $N(CH_3)_4NO_3$ using the four spectra shown in Fig. 5(b) as models did not show any major improvement compared to those obtained in Fig. 8 as shown in Fig. S9. This could be due to the high overlap among the component spectra.

In acetonitrile the high formation constant for $UO_2(NO_3)_3^-$ suggests a specific role of $N(CH_3)_4^+$ ion in promoting anionic complexation of uranyl, likely by the formation of an ion-association complex. The speciation of uranyl in aqueous and acetonitrile solutions containing $N(CH_3)_4^+$ share similarities based on: (1) increased spectral redshift in the presence of $N(CH_3)_4^+$ compared to other salts. Anionic complex formation in acetonitrile is accompanied by increased spectral intensity at higher wavelengths, (2) higher apparent formation constant for the mono-nitrate complex albeit with poorer fit compared to other alkali salts, and (3) increase in the lifetime of uranyl fluorescence at high concentration of $N(CH_3)_4^+$ and the corresponding increase in lifetime upon the formation of anionic complex in acetonitrile. Thus, we propose that ion-association complexes of uranyl with $N(CH_3)_4^+$ are formed in aqueous solutions as well. As water ($\varepsilon = 80.1$) is more polar compared to acetonitrile ($\varepsilon = 37.5$), formation of anionic complexes in water can be relatively suppressed. Similar ion-association interactions involving quaternary ammonium cations and actinyls has been suggested to a play role in the stability of actinyl chloro complexes.[35] A more detailed study of the photochemistry of uranyl in the presence of complexing ligands and structural

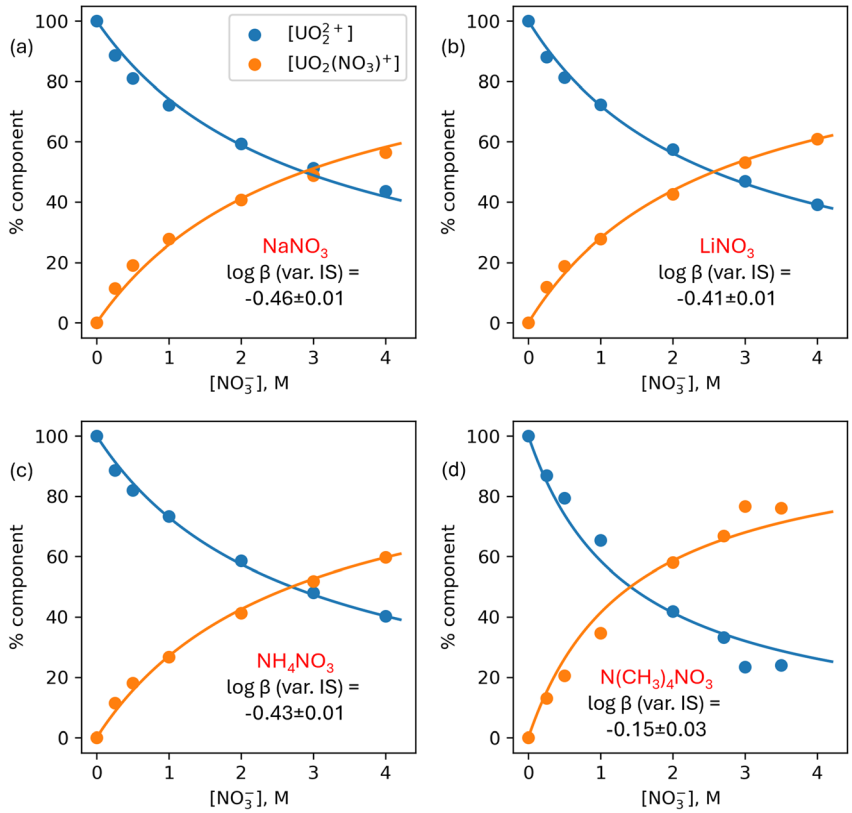

Fig. 9 Contributions of the two spectral components in different nitrate solutions obtained from fitting lifetime-corrected spectra to eqn (1c): (a) $NaNO_3$, (b) $LiNO_3$, (c) NH_4NO_3, and (d) $N(CH_3)_4NO_3$. The lines passing through the points are obtained by fitting the component fractions to the mass action model shown in eqn (3). Apparent formation constants (log β) obtained from the fits are shown on the panels for different nitrate salts.

Table 2 Fit values for the apparent formation constants with uncertainties obtained by fitting the component fractions to the mass-action model with two components according to eqn (3)

Salt	Log β
$NaNO_3$ + $NaClO_4$ (IS = 4 M)	-0.44 ± 0.01
$NaNO_3$ (var. IS)	-0.46 ± 0.01
$LiNO_3$ (var. IS)	-0.41 ± 0.01
NH_4NO_3 (var. IS)	-0.44 ± 0.01
$N(CH_3)_4NO_3$ (var. IS)	-0.16 ± 0.03

studies such as X-ray scattering of the solution species are needed to address the role of cations and solvents.[52,53]

Conclusions

We have shown that TRFLS can be used to quantify the speciation of uranyl in aqueous and acetonitrile solutions which contain nitrate salts. Since lifetimes of uranyl fluorescence were found to be highly sensitive to the solution medium without clear connections to the uranyl speciation, lifetime corrected spectra were used to obtain the speciation. In aqueous nitrate solutions, except those containing $N(CH_3)_4NO_3$, uranyl forms only UO_2^{2+} and $UO_2(NO_3)^+$ complexes, and not higher nitrate complexes. The low value of the apparent formation constant for the formation of mono-nitrate complex in these aqueous solutions agrees with the values reported in literature. In acetonitrile, di- and tris-nitrato species are observed, with near quantitative conversion to tris-nitrato species in the presence of 1 : 3 U(VI):nitrate. Aqueous solutions containing $N(CH_3)_4NO_3$ are distinct from other aqueous solutions with a higher redshift in the spectra and poorer fits to the two-component model. The corresponding component fractions are also not adequately captured by the formation of $UO_2(NO_3)^+$ alone. Attempts to include more components in the spectral fitting for the quat were not successful, possibly due to high overlap among the component spectra. The parallel aqueous/non-aqueous trends point to an ion-association mechanism in which quats stabilize the negatively charged uranyl complexes. These insights provide a molecular basis for designing quat-assisted separation and sensing technologies that selectively target anionic actinide species.

Conflicts of interest

There are no conflicts to declare.

Data availability

All the data used are provided in the manuscript and the supplementary information (SI). Supplementary information: fluorescence decay of U(IV) in aqueous solutions. TRLFS of

uranyl in $NaNO_3$ and $N(CH_3)_4NO_3$ solutions. Lifetimes for uranyl in $LiNO_3$ and NH_4NO_3 solutions. Lifetime corrected spectra of uranyl in $LiNO_3$ and NH_4NO_3 solutions. Fluorescence decay of U(IV) in acetonitrile with $N(CH_3)_4NO_3$. Lifetime spectra and Stern–Volmer plot for $UO_2(NO_3)_2 \cdot 6H_2O$ in acetonitrile solutions of $N(CH_3)_4NO_3$. Fits to $I^0(\lambda)$ for U(IV) in 3.5 M aqueous $N(CH_3)_4NO_3$ solution using two and four component models. See DOI: https://doi.org/10.1039/d5ra06251a.

Acknowledgements

This work was supported by the U.S. Department of Energy, Office of Basic Energy Science, Division of Chemical Sciences, Geosciences, and Biosciences, Separation Science program under contract DE-AC02-06CH11357. S. N. is grateful to Richard E Wilson for his encouragement and critical discussion of this work.

References

1 D. T. Reed, S. B. Clark and L. Rao, *Actinide Speciation in High Ionic Strength Media*, Springer, 1999.
2 K. L. Nash, C. Madic, J. N. Mathur and J. Lacquement, *The Chemistry of the Actinide and Transactinide Elements*, Springer, 2006, pp. 2622–2798.
3 K. Maher, J. R. Bargar and G. E. J. Brown, Environmental Speciation of Actinides, *Inorg. Chem.*, 2013, **52**, 3510–3532.
4 J. K. Gibson and W. A. de Jong, *Experimental and Theoretical Approaches to Actinide Chemistry*, John Wiley & Sons, 2018.
5 I. Grenthe and X. Gaona, *Second update on the chemical thermodynamics of uranium, neptunium, plutonium, americium and technetium*, OECD/NEA Publishing, 2020.
6 G. Anderegg, F. Arnaud-Neu, R. Delgado, J. Felcman and K. Popov, Critical evaluation of stability constants of metal complexes of complexones for biomedical and environmental applications (IUPAC Technical Report), *Pure Appl. Chem.*, 2005, **77**, 1445–1495.
7 S. B. Clark, M. Buchanan and B. Wilmarth, *Basic Research Needs for Environmental Management*, 2016.
8 Others, *et al.*, *Basic Energy Sciences Roundtable: Foundational Science to Accelerate Nuclear Energy Innovation*, 2024.
9 I. Grenthe, J. Fuger, R. J. Konings, R. J. Lemire, A. B. Muller; C. Nguyen-Trung and H. Wanner, *Chemical Thermodynamics of Uranium*, Elsevier, Amsterdam, 1992, vol. 1.
10 P. Danesi, R. Chiarizia, G. Scibona and G. D'Alessandro, Stability constants of nitrate and chloride complexes of Np (IV), Np (V) and Np (VI) ions, *J. Inorg. Nucl. Chem.*, 1971, **33**, 3503–3510.
11 K. Spahiu and I. Puigdomenech, On weak complex formation: re-interpretation of literature data on the Np and Pu nitrate complexation, *Radiochim. Acta*, 1998, **82**, 413–420.
12 A. Ikeda-Ohno, C. Hennig, A. Rossberg, H. Funke, A. C. Scheinost, G. Bernhard and T. Yaita, Electrochemical and complexation behavior of neptunium in aqueous perchlorate and nitrate solutions, *Inorg. Chem.*, 2008, **47**, 8294–8305.
13 A. J. Gaunt, I. May, M. P. Neu, S. D. Reilly and B. L. Scott, Structural and spectroscopic characterization of plutonyl (VI) nitrate under acidic conditions, *Inorg. Chem.*, 2011, **50**, 4244–4246.
14 P. Lindqvist-Reis, C. Apostolidis, O. Walter, R. Marsac, N. L. Banik, M. Y. Skripkin, J. Rothe and A. Morgenstern, Structure and spectroscopy of hydrated neptunyl (VI) nitrate complexes, *Dalton Trans.*, 2013, **42**, 15275–15279.
15 A. Ikeda-Ohno, C. Hennig, S. Tsushima, A. C. Scheinost, G. Bernhard and T. Yaita, Speciation and structural study of U (IV) and-(VI) in perchloric and nitric acid solutions, *Inorg. Chem.*, 2009, **48**, 7201–7210.
16 H. Lahr and W. Knoch, Bestimmung von stabilitätskonstanten einiger aktinidenkomplexe: II. Nitrat- und chloridkomplexe von uran, neptunium, plutonium und americium, *Radiochim. Acta*, 1970, **13**, 1–5.
17 G. R. Choppin and M. Du, f-Element Complexation in Brine Solutions, *Radiochim. Acta*, 1992, **58–59**, 101–104.
18 S. Ahrland, A. Tiselius and G. Ehrensvärd, On the Complex Chemistry of the Uranyl Ion. VI. The Complexity of Uranyl Chloride, Bromide and Nitrate, *Acta Chem. Scand.*, 1951, **5**, 1271–1282.
19 R. Betts and R. K. S. Michels, Ionic association in aqueous solutions of uranyl sulphate and uranyl nitrate, *J. Chem. Soc.*, 1949, S286–S294.
20 O. Suleimenov, T. M. Seward and J. Hovey, A spectrophotometric study on uranyl nitrate complexation to 150 C, *J. Solut. Chem.*, 2007, **36**, 1093–1102.
21 L. Rao and G. Tian, Thermodynamic study of the complexation of uranium (VI) with nitrate at variable temperatures, *J. Chem. Thermodyn.*, 2008, **40**, 1001–1006.
22 S. De Houwer and C. Görller-Walrand, Influence of complex formation on the electronic structure of uranyl, *J. Alloys Compd.*, 2001, **323**, 683–687.
23 N. A. Smith and K. R. Czerwinski, Speciation of the uranyl nitrate system via spectrophotometric titrations, *J. Radioanal. Nucl. Chem.*, 2013, **298**, 1777–1783.
24 K. L. Nash, A review of the basic chemistry and recent developments in trivalent f-elements separations, *Solvent Extr. Ion Exch.*, 1993, **11**, 729–768.
25 R. Lommelen, B. Onghena and K. Binnemans, Cation effect of chloride salting agents on transition metal ion hydration and solvent extraction by the basic extractant methyltrioctylammonium chloride, *Inorg. Chem.*, 2020, **59**, 13442–13452.
26 G. B. Jin, J. Lin, S. L. Estes, S. Skanthakumar and L. Soderholm, Influence of countercation hydration enthalpies on the formation of molecular complexes: a thorium–nitrate example, *J. Am. Chem. Soc.*, 2017, **139**, 18003–18008.
27 A. Lichtenberg, M. Zegke, G. S. Nichol, A. Raauf and S. Mathur, Influence of alkali metal cations on the formation of the heterobimetallic actinide tert-butoxides [AnM3(OtBu)7] and [AnM2(OtBu)6](AnIV = Th, U; MI= Li, Na, K, Rb, Cs), *Dalton Trans.*, 2023, **52**, 962–970.
28 M. C. Shore, J. N. Wacker, P. Miró, J. A. Bertke and K. E. Knope, Alkali Counterion-Dependent Crystallization of Uranium (IV)–Chloro Structural Units, *Inorg. Chem.*, 2025.

29 H.-W. Wang, T. R. Graham, E. Mamontov, K. Page, A. G. Stack and C. I. Pearce, Countercations control local specific bonding interactions and nucleation mechanisms in concentrated water-in-salt solutions, *J. Phys. Chem. Lett.*, 2019, **10**, 3318–3325.

30 N. Rampal, H.-W. Wang, D. Biriukov, A. B. Brady, J. C. Neuefeind, M. Předota and A. G. Stack, Local molecular environment drives speciation and reactivity of ion complexes in concentrated salt solution, *J. Mol. Liq.*, 2021, **340**, 116898.

31 G. Bernhard, G. Geipel, V. Brendler and H. Nitsche, Speciation of uranium in seepage waters of a mine tailing pile studied by time-resolved laser-induced fluorescence spectroscopy (TRLFS), *Radiochim. Acta*, 1996, **74**, 87–92.

32 M. Altmaier, X. Gaona and T. Fanghaanel, Recent advances in aqueous actinide chemistry and thermodynamics, *Chem. Rev.*, 2013, **113**, 901–943.

33 C. Musikas, Formation d'uranates solubles par hydrolyse des ions uranyle (VI), *Radiochem. Radioanal. Lett.*, 1972, **11**, 307–316.

34 L. Maya and G. Begun, A Raman spectroscopy study of hydroxo and carbonato species of the uranyl (VI) ion, *J. Inorg. Nucl. Chem.*, 1981, **43**, 2827–2832.

35 S. L. Estes, B. Qiao and G. B. Jin, Ion association with tetra-n-alkylammonium cations stabilizes higher-oxidation-state neptunium dioxocations, *Nat. Commun.*, 2019, **10**, 59.

36 K. Servaes, C. Hennig, I. Billard, C. Gaillard, K. Binnemans, C. Görller-Walrand and R. Van Deun, Speciation of Uranyl Nitrato Complexes in Acetonitrile and in the Ionic Liquid 1-Butyl-3-methylimidazolium Bis (trifluoromethylsulfonyl) imide, *Eur. J. Inorg. Chem.*, 2007, 5120–5126.

37 A. Ikeda, C. Hennig, A. Rossberg, S. Tsushima, A. C. Scheinost and G. Bernhard, Structural determination of individual chemical species in a mixed system by iterative transformation factor analysis-based X-ray absorption spectroscopy combined with UV- Visible absorption and quantum chemical calculation, *Anal. Chem.*, 2008, **80**, 1102–1110.

38 C. M. Starks, C. L. Liotta, M. E. Halpern, C. M. Starks, C. L. Liotta and M. E. Halpern, Phase-transfer catalysis: Fundamentals I, *Phase-Transfer Catalysis: Fundamentals, Applications, and Industrial Perspectives*, 1994, pp. 23–47.

39 Others, *et al.*, Aqueous solutions of uranium (VI) as studied by time-resolved emission spectroscopy: a round-robin test, *Appl. Spectrosc.*, 2003, **57**, 1027–1038.

40 B. Li, M. Bao, Y. Kang, L. Wang, Y. Liu, L. Wang and C. Xu, Hydrophilic chelators for coordination and separation of radioactive f-block elements, *Natl. Sci. Open*, 2025, **4**, 20240028.

41 M. Newville, T. Stensitzki, D. B. Allen and A. Ingargiola, *LMFIT: Non-linear Least-Square Minimization and Curve-Fitting for Python*, 2015,.

42 L. Couston, D. Pouyat, C. Moulin and P. Decambox, Speciation of uranyl species in nitric acid medium by time-resolved laser-induced fluorescence, *Appl. Spectrosc.*, 1995, **49**, 349–353.

43 I. Billard and K. Lützenkirchen, Equilibrium constants in aqueous lanthanide and actinide chemistry from time-resolved fluorescence spectroscopy: the role of ground and excited state reactions, *Radiochim. Acta*, 2003, **91**, 285–294.

44 N. Bardin, P. Rubini and C. Madic, Hydration of actinyl (VI), MO_{2aq}^{2+} (M = U, Np, Pu). An NMR study, *Radiochim. Acta*, 1998, **83**, 189–194.

45 L. Sémon, C. Boehme, I. Billard, C. Hennig, K. Lützenkirchen, T. Reich, A. Roßberg, I. Rossini and G. Wipff, Do perchlorate and triflate anions bind to the uranyl cation in an acidic aqueous medium? A combined EXAFS and quantum mechanical investigation, *ChemPhysChem*, 2001, **2**, 591–598.

46 C. Nguyen Trung, G. Begun and D. A. Palmer, Aqueous uranium complexes. 2. Raman spectroscopic study of the complex formation of the dioxouranium (VI) ion with a variety of inorganic and organic ligands, *Inorg. Chem.*, 1992, **31**, 5280–5287.

47 M. Autillo, R. E. Wilson, M. Vasiliu, G. F. de Melo and D. A. Dixon, Periodic Trends within Actinyl (VI) Nitrates and Their Structures, Vibrational Spectra, and Electronic Properties, *Inorg. Chem.*, 2022, **61**, 15607–15618.

48 R. Day Jr and R. Powers, Extraction of uranyl ion from some aqueous salt solutions with 2-thenoyltrifluoroacetone, *J. Am. Chem. Soc.*, 1954, **76**, 3895–3897.

49 A. Leung, L. Hayashibara and J. Spadaro, Fluorescence properties of uranyl nitrates, *J. Phys. Chem. Solids*, 1999, **60**, 299–304.

50 T. Bäcker and A.-V. Mudring, Sodium Trinitratouranylate(VI) Na[UO2(NO3)3], *Z. Anorg. Allg. Chem.*, 2010, **636**, 1002–1005.

51 S. Kumar, S. Maji, K. Sundararajan and K. Sankaran, Uranyl tris nitrato as a luminescent probe for trace water detection in acetonitrile, *Luminescence*, 2018, **33**, 611–615.

52 L. Soderholm, S. Skanthakumar and R. E. Wilson, Structural correspondence between uranyl chloride complexes in solution and their stability constants, *J. Phys. Chem. A*, 2011, **115**, 4959–4967.

53 S. Skanthakumar, G. B. Jin, J. Lin, V. Vallet and L. Soderholm, Linking Solution Structures and Energetics: Thorium Nitrate Complexes, *J. Phys. Chem. B*, 2017, **121**, 8577–8584.